Growth of compact arrays of optical quality single crystalline ZnO nanorods by low temperature method

MANORANJAN GHOSH, RITWIK BHATTACHARYYA and A K RAYCHAUDHURI*

DST Unit for Nanoscience, S.N. Bose National Centre for Basic Sciences, Kolkata 700 098, India

Abstract. We report the synthesis and optical properties of compact and aligned ZnO nanorod arrays (dia, ~50–200 nm) grown on a glass substrate with varying seed particle density. The suspension of ZnO nanoparticles (size, ~15 nm) of various concentrations are used as seed layer for the growth of nanorod arrays via self-assembly of ZnO from solution. We studied the effect of various growth parameters (such as seeding density, microstructure of the seed layer) as well as the growth time on the growth and alignment of the nanorods. We find that the growth, areal density and alignment of the nanorods depend on the density of seed particles which can be controlled. It is observed that there is a critical density of the seed particles at which nanorod arrays show maximum preferred orientation along [002] direction. The minimum and maximum radius of the aligned nanorods synthesized by this method lie in the range 50–220 nm which depend on the seeding density and time of growth. These nanorods have a bandgap of 3·3 eV as in the case of bulk crystals and show emission in the UV region of the spectrum (~400 nm) due to excitonic recombination and defect related emission in the visible region.

Keywords. ZnO; nanorods; density controlled growth; preferred orientation.

1. Introduction

In recent years, ZnO has emerged as one of the most studied materials. This is a wide bandgap semiconductor having wurtzite structure. ZnO has promising applications in many optoelectronic and sensing devices such as UV lasing (Sun *et al* 2003), transparent conduction electrodes (Minami 2005) and gas sensors (Ding *et al* 2005). These application prospects depend on the successful fabrication of a variety of ZnO microstructures/nanostructures for specific purposes. One of the important physical forms of ZnO nanostructures that have attracted considerable attention is the one-dimensional (1D) nanorods. Formidable amount of research work has been done on synthesizing 1D nanostructures of ZnO using different routes (Wang *et al* 2001; Kind *et al* 2002; Pacholski *et al* 2002). Recently, 2D periodic array of ZnO micro-rods and micro-tunnels have been demonstrated (Kim *et al* 2006). This kind of carefully regulated nanostructures can find applications as a biosensor (Dorfman *et al* 2006) and optimum generation of green oxidizer, H_2O_2, by photocatalytic reaction (Jang *et al* 2006). With a large exciton binding energy and high melting temperature, ZnO nanowires have been studied as field emission source (Lee *et al* 2002; Banerjee *et al* 2004; Ramgir *et al* 2006). Optimization of their field emission properties has been recently demonstrated by controlling the density of ZnO

nanowire arrays through vapour–solid–liquid (VLS) growth process (Xudong *et al* 2007).

A cost effective method to grow large aligned arrays of ZnO nanorods is a low temperature chemical method (Greene *et al* 2003). This method which uses a seed layer of ZnO nanoparticles to nucleate the growth process falls in the general class of nanostructure growth through site specific nucleation. In this method, areal density of the random array of nucleation sites provides an easy way to control the density and overall orientation of the nanorod arrays (Ma *et al* 2007).

An important challenge in this method of growth is the optimization of preferred orientation as well as the size of the nanorod arrays by controlling the density of the seed nanoparticles. In this paper, we address this specific issue which has not been addressed to in detail in earlier publications in this field. The purpose of the paper is to establish the different growth parameters and how they control the growth of the array and the alignment of the nanorods. We study the effect of seeding density, the microstructure of the seeding layer as well as the growth time on the growth and alignment of the nanorods.

We note that the synthesis of microstructures/nanostructures of ZnO by hydrothermal/chemical method has already proven to be advantageous because of its low cost, freedom from strain and morphology controllable extended area synthesis compared to the other vapour phase methods like evaporation and condensation (Park *et al* 2003; Zhang *et al* 2005), physical vapour deposition (Li *et al* 2004; Kumar *et al* 2005) and chemical vapour deposition (Kim *et al* 2004; Hirate *et al* 2005). In the hydrothermal

---

*Author for correspondence (arup@bose.res.in)

method, the morphology of the ZnO crystals can be easily controlled by varying the growth conditions such as growth time (Chander and Raychaudhuri 2006), growth temperature (Chen *et al* 1999), pH (Lu and Yeh 2000), and absorbing molecules (Cao *et al* 2004). The resulting nanocrystals show different optical properties depending on their growth conditions (Guo *et al* 2005; Shalish *et al* 2004). Optimization of growth parameters for the aligned arrays of nanorods by this method is the principal motivation of this work.

2. Experimental

2.1 *Growth protocol*

A two-step process has been followed to grow the ZnO nanorods from ZnO seed particles in this low temperature method (Pacholski *et al* 2002; Chander and Raychaudhuri 2006). In the first step, we have synthesized ZnO nanoparticles of diameter, ~ 15 nm, to use them as a seed layer on a glass substrate. In the second step, ZnO nanorods have been grown on the seeded layer as described below.

Step I: ZnO nanocrystals to be used as seed layer have been synthesized by acetate route as described elsewhere (Ghosh and Raychaudhuri 2006, 2007). Briefly, 50 mM zinc acetate dihydrate and 100 mM NaOH solution in ethanol were reacted for 6 h at temperature, 70–75°C, to produce ZnO nanocrystals of size, 15 nm. Our objective was to control the density of the nanorods that were grown on these seeds. The density of the rods grown depend on the density of the seed particles. To grow the nanorod arrays with controlled density, we have prepared ZnO nanoparticles suspended in ethanol with different concentrations over a wide range (3 orders). This was done by the method of evaporation and dilution of the mother solution obtained as described above. For the labeling purpose nanoparticle suspensions were assigned by the strength of relative concentrations. The mother ZnO suspension corresponding to the $Zn(CH_3COO)_2, 2H_2O$ concentration of 50 mM was assigned as 1. Relative concentrations of 0·01 and 0·1 were achieved by 100 and 10 times dilution, respectively. Relative concentration higher than 1, such as 5 and 10 were achieved by maintaining the final volume at 1/5th and 1/10th of the initial volume of the mother solution by the method of evaporation. These nanocrystal suspensions were then used to produce a seed layer of different seed particle density by dip coating on a glass substrate.

Prior to seeding the substrate was cleaned by following the standard RCA cleaning procedure to make the surface hydrophilic. The seeded substrates were heat treated for 1 h at a temperature of 120°C for better adhesion of the seed particles to the substrate. The seed layers thus prepared, act as nucleating sites leading to aligned growth of nanorods. It is important to realize, as we will show below that the seed layer thus formed has varying microstructures

and that changes the growth pattern of the rods. We study and characterize the microstructure and show that the size and density of the rods grown depend on the nature of the microstructure of starting seed layer.

Step II: The glass substrates seeded with the nanoparticles suspension of various relative concentrations were placed upside down inside a beaker containing an aqueous solution of 30 mM zinc nitrate hexahydrate and 30 mM hexamethylenetetramine (HMT) solution in water kept at 95°C. Synthesis of aligned nanorod arrays on the substrate was performed by keeping it inside the solution for 3·5, 5 and 10 h with constant stirring. Since the seed particles act as nucleating site, seed layers of different areal density of the seed particles produce nanorod arrays of different density. After desired time of growth, the samples were taken out of the solution, rinsed with deionized water and dried in an oven preset at 120°C.

2.2 *Characterization methods used and optical measurements*

The principal characterization tools used are transmission electron microscope (TEM), scanning electron microscope (SEM) and X-ray diffraction (XRD). The nanoparticles were imaged and their lattice images were taken with a JEOL high-resolution transmission electron microscopy (HR-TEM) at 200 keV. The seed layer and the nanorod arrays grown on them were analysed through scanning electron microscope (SEM). The X-ray diffraction data were collected by a Philips X'pert Pro X-ray diffractometer. Room temperature optical properties were studied by photoluminescence spectrometer (Jobin Yvon, FluoroMax-3) where a xenon arc lamp was used as illumination source.

3. Results and discussion

3.1 *Important growth parameters and quality of rods grown*

This paper is focused on the growth process for the nanorods and the important parameters that need be varied to get control on the diameter and alignment of the rods. In this subsection we establish these parameters and also show the structural as well as optical quality of the rods grown by this method.

From an analysis of the growth process as described below we make the hypothesis that there are two important factors in the growth process that make crystallographically aligned nanorods. The first factor is the anisotropy in the growth rate of ZnO for different crystal faces which determines the morphology as well as the aspect ratio of the crystal (Garcia and Semancik *et al* 2007). In this crystal, the *c*-axis has the fastest direction of growth and in any growth process growth along this direction wins over. Thus one obtains nanorods which

have their growth axis along the *c*-axis. [Note: In our previous study, (Chander and Raychaudhuri 2006), we have shown that the grown rods have a limiting average aspect ratio (length/diameter) ≈ 7]. The second issue is that of alignment of the grown rods. We propose that the alignment of the grown rods is mainly from 'crowding' effect which limits axial growth of the rods parallel to the substrate. We explain this in subsection 3·3 below.

In the present study, unmodified surface of the glass substrate has been pre-coated by a seed layer of ZnO nanoparticles. TEM image of nanoparticles used is shown in figure 2(a). It is the same material as the nanorods to be grown and so provides a homogeneous nucleation site for the growth of ZnO nanorods. Seeding the substrate by the nanocrystals is an effective way to control the orientation of the deposited crystals. Site-specific nucleation at the seed particles is essential to obtain aligned nanorod arrays perpendicular to the substrate. In this investigation, we wanted to establish the extent to which the areal density of the seed particles is a key factor in determining the overall orientation of the nanorod arrays. This will be discussed in the next section.

Longer growth time results in better alignment along the direction perpendicular to the substrate. The XRD patterns of the nanorod arrays grown on a seed layer of relative concentration 0·1 for 10 h (figure 1) shows a single peak due to the reflection from (002) planes. Nanorod arrays grown for 5 h on seed layer of similar concentration show almost all the peaks of wurtzite ZnO. However, the intensity profile is radically different from a powder diffraction pattern.

Growth of ZnO nanorods is also possible on an unseeded surface. But these nanorods are not at all aligned in a certain direction and they follow a random growth pattern. This fact is also reflected in the XRD results indicated in figure 1. The intensity ratios of (100) and (002) peaks to the highest intensity peak (101) of wurtzite ZnO (indexed in figure 1) agree well with the bulk ZnO (zinc white) values of 0·71 and 0·56, respectively, which confirms the random orientation of the nanorods grown on the substrate. Since the seed crystal provides a homogeneous nucleation site, which has (002) planes parallel to the substrate, further deposition occurs along [002] direction perpendicular to the substrate. On the other hand, unseeded surface provides heterogeneous nucleation sites (Vayssieres *et al* 2001) which has complex nature and prompts growth of nanorods along random directions as discussed in §3.2.

These nanorods grown by the low temperature growth method are crystalline and show good optical properties. The lattice image of the nanorods shown in figure 2(b) is depicted in figure 2(c). The distance between lattice fringes is 2·66 Å which confirms the nanorods growth along [002] direction. The indexed SAED pattern confirms single crystalline nature of the hexagonal ZnO nanorods as shown in figure 2(d).

This paper is mainly focussed on the growth process and the growth parameters. However, we present the photoluminescence (PL) data of the nanorods grown by this method to establish that they have the desirable optical properties. Though a detailed discussion on the optical property is beyond the scope of this paper, we will briefly mention some of the observations on the optical properties of the nanorods grown.

In our study, ZnO nanorods arrays (as well as the seed layer) primarily show the near band edge emission at around 400 nm when excited by a wavelength of 325 nm. As a typical example, the PL spectrum of nanorod arrays corresponding to relative concentration 1, is shown in figure 3. The emission spectrum is broad and it extends in the visible and there is a shallow shoulder in the emission spectra around 560 nm. The observed spectrum can be resolved into three distinct peaks when fitted by multi peak fitting procedure as shown in figure 3. These three peaks have different origins. The sharp emission at 399 nm occurs due to free excitonic recombination which reflects the intrinsic nature of bulk ZnO. In addition to that the luminescence band near 432 nm is due to the excitons localized at the surface centres known as surface exciton (Travnikov *et al* 1990). One more broad and structureless emission band commonly observed in ZnO nanostructures (Shalish *et al* 2004) appears in our study near the green–orange (564 nm) region. The origin of this emission
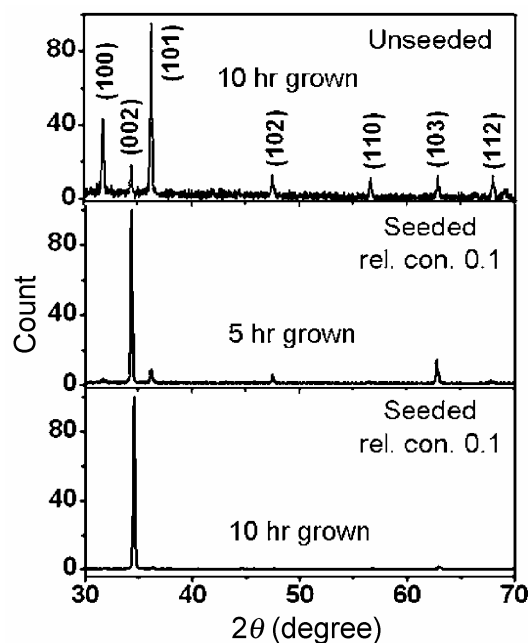

Figure 1. XRD data of the ZnO nanorods for the growth condition as indicated on the graph. The lower and middle panels show the XRD data for 10 h and 5 h grown samples, respectively. The relative concentration of seed particle is 0·1 for both the cases. Preferred growth along [002] direction is higher in case of longer growth time. The top panel shows the XRD data of ZnO nanorods grown on an unseeded surface.
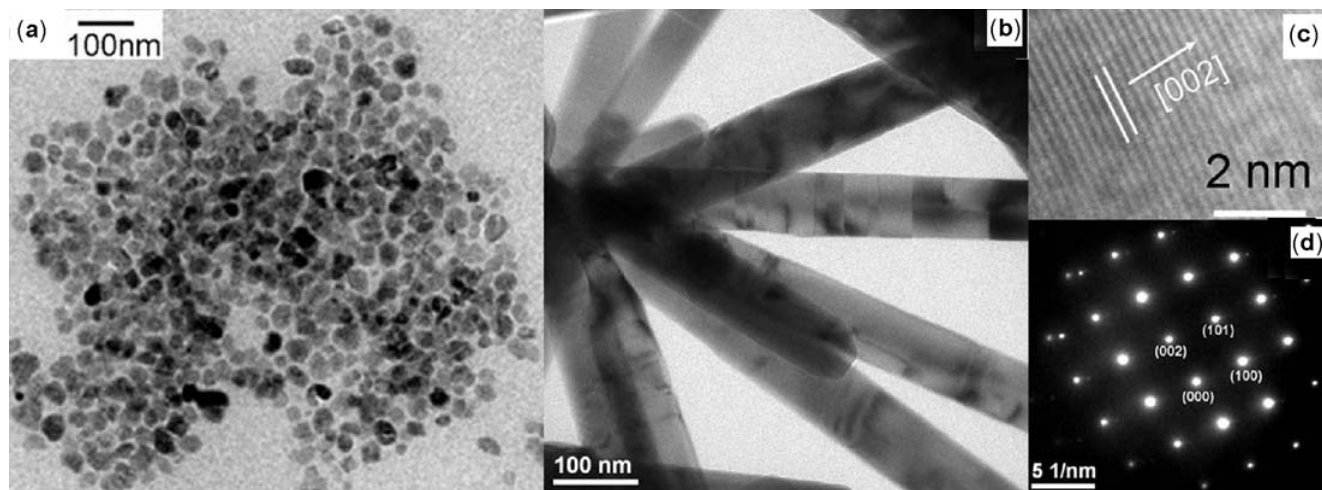
Figure 2. (**a**) TEM image of the seed nanoparticles taken on a grid from a suspension in ethanol, (**b**) TEM image of ZnO nanorods grown for 5 h, (**c**) lattice image of the nanorods. The distance between lattice fringes is 2·66 Å which confirms the nanorods growth along [002] direction and (**d**) the indexed SAED pattern of the nanorods confirms the hexagonal symmetry of the single crystalline ZnO nanorod.
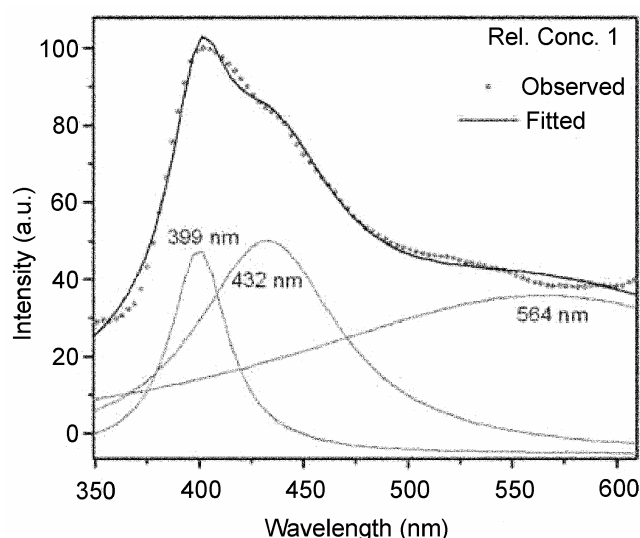

Figure 3. PL spectrum (excitation wavelength, ∼ 325 nm) of ZnO nanorods grown on a seed layer of relative concentration, 1 for 5 h.

is a matter of debate (Djurisic *et al* 2007) but broadly accepted as related to donors–deep acceptor (zinc and oxygen vacancy) transition (Heo *et al* 2005). The intensity of the visible emission depends on the size of the nanorods and it increases as the size is reduced.

3.2 *Effect of areal density and size of seed particles on grown ZnO nanorods*

In the growth of nanorod arrays by site specific homogeneous nucleation via seeding of the substrate, it is expected that the density of the seed particles should have a

close correlation with the density of the nanorods grown on them. This particular aspect, however, has not been investigated in quantitative details before. In our experiment, we study this specific issue. Also the minimum and maximum size of the grown nanorods have been determined.

The important point that emerges from our investigation is that there is no one–to–one relation between the number of nanoparticles and the number of nanorods grown. The number of seed particles is always much larger than the number of the aligned rods. The ideal situation where one nanorod growth takes place from a single seed particle is not valid. This would have happened if each of the seed particles will be oriented in one direction and all of them act as a nucleus. To examine the actual scenario, we have performed analysis of seeding layers with four different densities and the nanorods arrays grown on them. (The seed layer has random crystallographic orientation as confirmed by XRD). From this analysis we observe that processes like dip coating or spin coating of the substrate by the nanoparticles solution do not produce a uniform seed layer of same seed particle diameter as in the suspension. There is formation of aggregate that accompanies these coating processes as the particles are not capped. TEM image of a collection of seed particles (figure 2(a)) taken from the suspension, reveals a narrow diameter distribution with mean value around 15 nm. But the seed layer on the substrate produced after dip coating of the same particles, followed by heat treatment for 1 h at 120°C, shows that the seed particles get agglomerated and formation of multiple layers of seed particles is observed for higher concentration.

Figures 4(a), (b) and (c) show the SEM images of seeded layers for seed particle relative concentrations (see §2) of
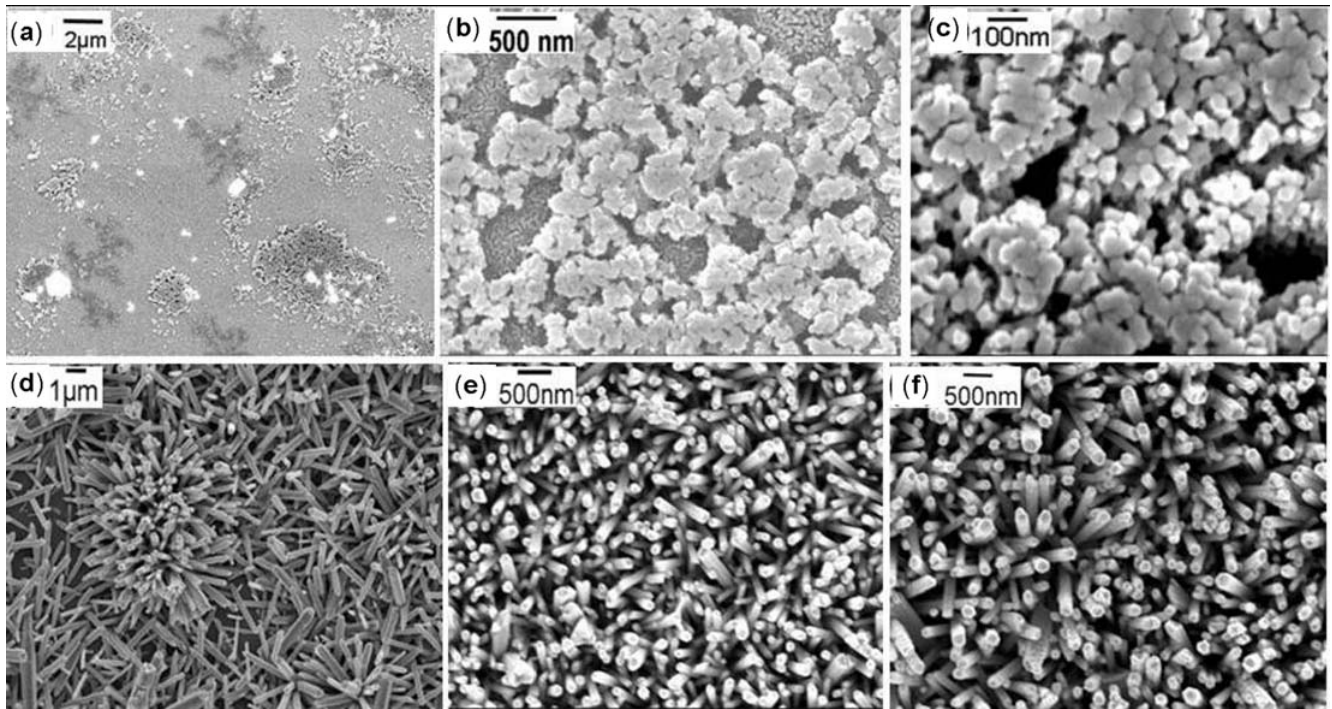
Figure 4. SEM images of ZnO seed particles dip coated onto the glass substrates and the nanorods arrays grown on them for 5 h. (**a**), (**b**) and (**c**) are the SEM images of seeded layers having relative concentrations of seed particles, 0·01, 1 and 10, respectively. (**d**), (**e**) and (**f**) are the top view of the nanorods arrays grown on (**a**), (**b**) and (**c**), respectively.

Table 1. Density and diameters of the nanorods grown for 5 h on seed layer of different concentrations.

Relative concentration of seed particles	Rod density (μm^{-2})	Rod diameter (nm)	$I_{(002)}/I_{(101)}$
0·01	No aligned rods	150–220 length ~ 2 μm	1·9
0·1	41	50–150	22·9
1	60	50–100	226·7
10	45	75–175	108·6

0·01, 1 and 10, respectively and (d), (e) and (f) are the respective nanorod arrays grown on them for 5 h. In table 1 we collect the relevant data. In the last column, we show the ratio $I_{(002)}/I_{(101)}$ which is the ratio of the intensities of the (002) and (101) lines in the XRD data and is a measure of the alignment. Higher the ratio, better is the alignment of the grown rods in the (002) direction. Dip coating of lowest concentration (relative concentration, 0·01) seed particles on a large area produce highly discontinuous seed layer (figure 4(a)). Major part of the surface does not have any seed nanocrystals. This prompts growth of nanorods in random direction on most part of the substrate as shown in figure 4(d). For higher relative concentration such as 1 and 10 shown in figures 4(b) and (c), improved continuity of the seed layer is observed. Formation of multiple layers of the seed particles is seen for relative concentration 10 as shown in figure 4(c). Figures 4(d), (e) and (f) show compact growth of nanorods on

these seed layers. As discussed in the next section, formation of multiple layers has implication on the preferred orientation of nanorod arrays grown on them. However, the number density of rods is maximum for the nanorods arrays (figure 4(e)) grown on almost uniform single layer of seed particles, corresponding to relative concentration 1 (see table 1). Smaller number density as well as poorer alignment (see table 1) is observed for nanorods grown on seed layers of relative concentration higher or lower than 1.

Analysis of the growth data shows that the average diameter of the nanorods grown increases when the density of the nanorods decreases. It is due to the fact that lateral growth of the nanorods gets limited by the surrounding nanorods due to crowding effect when the density is higher. It is interesting to note that the grain sizes of the agglomerated seed particles after dip-coating on the substrate is ≈ 40–50 nm although the exact size of the

nanocrystal in the suspension was found to be ≈ 15 nm (see the TEM image in figure 2(a)). Thus there is clear evidence of agglomeration on coating the seed particles. Because of this reason, ZnO nanorod arrays grown on such type of seeded layer is almost always greater than 40 nm (Greene *et al* 2003) and rod diameter < 40–50 nm obtained by seeded growth is rarely reported even when one starts with crystals of smaller size.

Nanorods have relatively higher average diameter (although with poorer alignment) on a seed layer of very low particle density (figure 4(e)) which contains large surface area depleted of seed particles as in the case of relative concentration, 0·01 (table 1). This confirms that the upper limit of the diameter of the nanorods grown has a dependence on the average separation of distinct nucleation site. A lower average density gives more space for lateral growth and hence larger diameter of the nanorods although absence of crowding leads to poor alignment.

3.3 *Control of preferred orientation of ZnO nanorod array*

The introduction of ZnO seed layers of different concentrations on the substrate not only controls the rod density but also has a strong impact on the orientation of the nanorod arrays. However, the preferential growth of ZnO nanorods along [002] direction is reported to increase as the seed particle density increases (Ma *et al* 2007). But in this report we show that there is a critical density of the seed particles for which the preferred orientation in [002] direction is maximum for a given growth time. A clear analysis of the preferential growth along [002] direction is possible if we follow the ratio of intensity of the (002) peak to intensity of the peak (101). [Note: In ZnO powder diffraction pattern, the highest intensity peak is the (101) peak]. The ratio, $I_{(002)}/I_{(101)}$, is a good measure of the orientation alignment of the nanorods. In figure 5, we plot the intensity ratio, $I_{(002)}/I_{(101)}$, for 3·5 and 5 h grown ZnO nanorod arrays. It can be clearly seen that there is a critical concentration of ZnO seed particles (relative concentration, 1) for which preferred orientation of ZnO nanorods along [002] direction is maximum. The ratio first increases as we increase the seed particle density (up to relative concentration, 1) and again decreases for higher values of seed particle densities (up to relative concentration, 10 has been shown). Much higher value of $I_{(002)}/I_{(101)}$ for 5 h grown nanorod arrays compared to 3·5 h grown rods is expected for obvious reason since longer growth time results in better alignment.

A plausible explanation for the existence of a critical density in the oriented growth is given below. At very low concentration of the starting solution, the coverage is low and there are islands of seed particles but a good fraction of the surface being exposed, it provides sites for heterogeneous nucleation that leads to random growth.

As the coverage increases smooth layer forms a smooth film, one obtains better orientation as the nucleation takes place from the large number of homogenous nucleation sites. At higher coverage the films become less smooth due to formation of a second layer that is not complete and there are sites where there are larger aggregates of the seed particles. This leads to large undulation (crest and trough) on the surface. The part of the exposed surface of seed layers parallel to the substrate (top of the crest and bottom of the trough), contains seed nanoparticles with exposed top surface which has (002) plane parallel to the substrate which leads to aligned nanorods perpendicular to the substrate. But at the walls of the crest, the exposed part of the seed particles is not parallel to the substrate and the growth from these sites can be random leading to gradual reduction of the alignment.

For the unseeded surface the density of the growing nanorods is low. In this case though the growth preferentially occurs in the [002] direction, the wires are mostly lying down on the substrate with random orientation. However, for the seeded surface the areal density is larger. The alignment in the direction perpendicular to the substrate happens due to crowding effect that prevents axial growth parallel to the substrate and the alignment generally becomes better as the growth time progresses. Thus the alignment of the nanorods as well as the aspect ratio depends on the growth time and the initial seeding density, which are the two important controllable parameters involved in the growth of nanorods. Both these factors in tandem decide the intimate extent of orientation achieved.
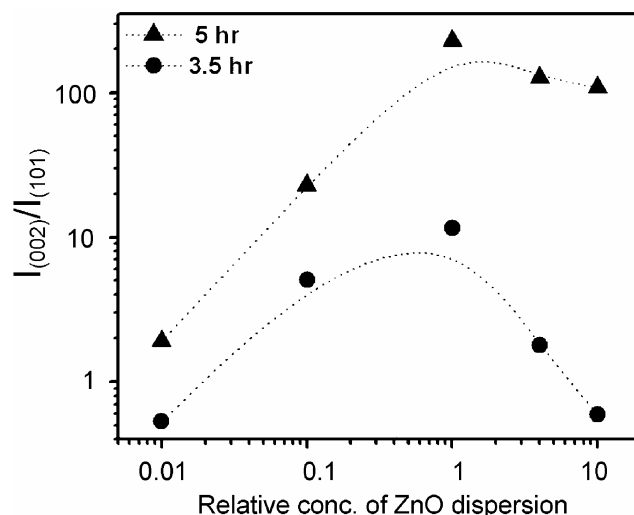

Figure 5. The intensity ratio between the peaks due to (002) and (101) reflections in the XRD data is plotted against the relative concentration of seed particles for the nanorod arrays grown for 3·5 and 5 h as indicated in the figure. There is a critical concentration of the seed particles (relative concentration 1) when the preferred growth along [002] direction is maximum.

4. Conclusions

We have successfully grown the density controlled ZnO nanorod arrays on seeded layers by a two-step low temperature method. The overall orientation of the nanorod arrays has been observed to be dependent on the density of the seed particles. The nature of the growth processes of the controlled nanorods arrays have been studied through SEM and XRD analyses. It is observed that there is a critical density of the seed particles (relative concentration 1, corresponding to 50 mM zinc acetate dihydrate solution) at which nanorod arrays show maximum preferred orientation along [002] direction. These nanorod arrays are single crystals and show good optical quality.

Acknowledgements

References

Banerjee D, Jo S H and Ren Z F 2004 *Adv. Mater.* **16** 2028

Cao M H, Guo C X, Qi Y J, Hu C W and Wang E B 2004 *J. Nanosci. Nanotechnol.* **4** 829

Chander R and Raychaudhuri A K 2006 *J. Mater. Sci.* **41** 3623

Chen D R, Jiao X L and Cheng G 1999 *Solid State Commun.* **113** 363

Ding G Q, Zheng M J, Xu W L and Shen W Z 2005 *Nanotechnology* **16** 1285

Djurisic A B *et al* 2007 *Nanotechnology* **18** 095702

Dorfman A, Kumar N and Hahm J 2006 *Adv. Mater.* **18** 2685

Garcia S P and Semancik S 2007 *Chem. Mater.* **19** 4016

Ghosh M and Raychaudhuri A K 2006 *J. Appl. Phys.* **100** 034315

Ghosh M and Raychaudhuri A K 2007 *Nanotechnology* **18** 115618

Guo M, Diao P and Cai S 2005 *J. Solid State Chem.* **178** 1864

Greene L E, Law M, Goldberger J, Kim F, Johnson J C, Zhang Y, Saykally R J and Yang P 2003 *Angew. Chem. Int. Ed.* **42** 3031

Heo Y W, Norton D P and Pearton S J 2005 *J. Appl. Phys.* **98** 073502

Hirate T, Sasaki S, Li W C, Miyashita H, Kimpara T and Satoh T 2005 *Thin Solid Films* **487** 35

Jang E S, Won J H, Hwang S J and Choy J H 2006 *Adv. Mater.* **18** 3309

Kim J H, Andeen D and Lange F F 2006 *Adv. Mater.* **18** 2453

Kim T Y, Kim J Y, Lee S H, Shim H W, Lee S H, Suh E K and Nahm K S 2004 *Synth. Met.* **144** 61

Kind H, Yan H Q, Messer B, Law M and Yang P D 2002 *Adv. Mater.* **14** 158

Kumar S, Gupta V and Sreenivas K 2005 *Nanotechnology* **16** 1167

Lee C J, Lee T J, Lyu S C, Zhang Y, Ruh H and Lee H J 2002 *Appl. Phys. Lett.* **81** 3648

Li S Y, Lin P, Lee C Y, Ho M S and Tseng T Y 2004 *J. Nanosci. Nanotechnol.* **4** 968

Lu C H and Yeh C H 2000 *Ceram. Int.* **26** 351

Ma T, Guo M, Zhang M, Zhang Y and Wang X 2007 *Nanotechnology* **18** 035605

Minami T 2005 *Semicond. Sci. Technol.* **20** S35

Pacholski C, Kornowski A and Weller H 2002 *Angew. Chem. Int. Ed.* **41** 1188

Park J, Choi H H, Siebein K and Singh R K 2003 *J. Cryst. Growth* **258** 342

Ramgir N S, Mulla I S, Vijayamohanan K, Late D J, Bhise A B, More M A and Joag D S 2006 *Appl. Phys. Lett.* **88** 042107

Shalish I, Temkin H and Narayanamurti V 2004 *Phys. Rev.* **B69** 245401

Sun X W, Yu S F, Xu C X, Yuen C, Chen B J and Li S 2003 *Jpn. J. Appl. Phys.* **42** L1229

Travnikov V V, Freiberg A and Savikhin S F 1990 *J. Lumines.* **47** 107

Vayssieres L, Keis K, Hagfeldt A and Lindquist S-E 2001 *Chem. Mater.* **13** 4395

Wang J F, Gudiksen M S, Duan X F, Cui Y and Lieber C M 2001 *Science* **293** 1455

Wang Xudong, Zhou J, Lao C, Song J, Xu N and Wang Z L 2007 *Adv. Mater.* **19** 1627

Zhang Y S, Wang L S, Liu X H, Yan Y J, Chen C Q and Zhu J 2005 *J. Phys. Chem.* **B109** 13091